

**Band Jahn-Teller structural phase transition in  $Y_2In$** E. Svanidze,<sup>1,\*</sup> C. Georgen,<sup>1</sup> A. M. Hallas,<sup>1</sup> Q. Huang,<sup>2</sup> J. M. Santiago,<sup>1</sup> J. W. Lynn,<sup>2</sup> and E. Morosan<sup>1</sup><sup>1</sup>*Department of Physics and Astronomy and Rice Center for Quantum Materials, Rice University, Houston, Texas 77005, USA*<sup>2</sup>*NIST Center for Neutron Research, National Institute of Standards and Technology, Gaithersburg, Maryland 20899, USA*

(Received 29 May 2017; revised manuscript received 6 December 2017; published 23 February 2018; corrected 25 May 2018)

The number of paramagnetic materials that undergo a structural phase transition is rather small, which can perhaps explain the limited understanding of the band Jahn-Teller mechanism responsible for this effect. Here we present a structural phase transition observed in paramagnetic  $Y_2In$  at temperature  $T_0 = 250 \pm 5$  K. Below  $T_0$ , the high-temperature hexagonal  $P6_3/mmc$  phase transforms into the low-temperature orthorhombic  $Pnma$  phase. This transition is accompanied by an unambiguous thermal hysteresis of about 10 K, observed in both magnetic susceptibility  $M/H(T)$  and resistivity  $\rho(T)$ , indicating a first-order transition. Band structure calculations suggest a band Jahn-Teller mechanism, during which the degeneracy of electron bands close to the Fermi energy is broken. We establish that this structural phase transition does not have a magnetic component; however, the possibility of a charge density wave formation has not been eliminated.

DOI: [10.1103/PhysRevB.97.054111](https://doi.org/10.1103/PhysRevB.97.054111)**I. INTRODUCTION**

A structural phase transition can be driven by a number of parameters—temperature [1–6], pressure [7], chemical composition [8,9], or magnetic field [10,11]. When the driving parameter is temperature, the transition typically occurs from a higher to a lower symmetry [12]. This is illustrated by a large number of austenite-martensite structural phase transitions, in which the high-temperature cubic phase is transformed into a low-temperature tetragonal one [4]. If the symmetry of two phases is different, the structural phase transition is likely to be first order, resulting in a discontinuous volume change. A reliable indicator of a first-order phase transition is the presence of hysteresis [13–15]. For temperature-induced transitions, the high- and low-temperature phases coexist in the region corresponding to the width of the hysteresis—in some materials, this region can be as small as a fraction of a Kelvin [16], while in others it can reach several hundreds of Kelvin [3,4,6,17]. Materials with wide thermal hystereses are frequently used as a basis for shape-memory devices [14].

Structural phase transitions are frequently accompanied by various phenomena. In magnetic compounds, structural phase transitions often accompany magnetic ordering [1,2,5,9,18]. In metals, charge transfer between various atoms can result in a change of valence, e.g., Mn- and Fe-based materials [14,19], that can lead to a metal-insulator transition [20]. The formation of a spin [21] or charge [22–24] density wave has also been associated with structural distortions. The origin of a structural instability in transition metals has been attributed to either a cooperative Jahn-Teller distortion (in systems with local moments) or a band Jahn-Teller effect (in systems without local moments) [12,25,26]. In the band Jahn-Teller model,

the lattice distortion breaks the degeneracy of the electron bands in the vicinity of the Fermi energy, which results in a redistribution of electrons between these bands, lowering the free energy [26]. The occurrence of a structural phase transition within the band Jahn-Teller model is suggested to arise in compounds for which there exists a sharp  $d$ -electron dominated peak close to the Fermi energy,  $E_F$ , which is either flattened or split into two peaks as a result of a structural phase transition [27–29]. Experimental realizations of this model include YCu [30] and LaCd [28].

While the majority of the  $R_2In$  compounds crystallize in the hexagonal  $P6_3/mmc$  structure [31,32], some are known to occur in the  $Pnma$  space group [33,34]. This, together with a large peak in the density of states (DOS) close to the Fermi energy  $DOS(E_F)$  [35], suggests the possibility of a band Jahn-Teller transition in  $Y_2In$ . In this paper, we present evidence for a structural phase transition from the high-temperature  $P6_3/mmc$  to a low-temperature  $Pnma$  phase in  $Y_2In$ . The transition is signaled by a step in the temperature-dependent susceptibility  $M(T)/H$  as well as resistivity  $\rho(T)$  around  $T_0 = 250 \pm 5$  K. In both measurements, a well-pronounced hysteresis of about 10 K suggests that the transition is first order, consistent with an abrupt volume change. Band structure calculations reveal the expected flattening of the  $d$ -electron peak in the DOS ( $E_F$ ).

**II. EXPERIMENTAL METHODS**

Several polycrystalline samples were synthesized by arc-melting Y (Hefa Rare Earths, 99.9%) and In (Alfa Aesar, 99.9995%) in ratios ranging from 1.8:1 to 2.3:1 with mass losses of no more than 0.5%. The arc-melted buttons were then wrapped in Ta foil and annealed at 950, 850, and 750 °C for 96 hours each. Both annealed and nonannealed samples are extremely air sensitive, similar to other  $R$ -In compounds [31]. All thermodynamic and transport measurements show

\*Present address: Max Planck Institute for Chemical Physics, Dresden, Germany.

TABLE I. Summary of parameters for the two  $Y_2In$  phases.

Space group	Lattice parameters			Volume ( $\text{\AA}^3$ )	$\chi$ (high $T$ , low $H$ ) ( $10^{-4}$ emu/mol $_{FU}$ )	$\chi_0 = \mu_B^2 \text{DOS}(E_F)$ ( $10^{-4}$ emu/mol $_{FU}$ )
	$a$ ( $\text{\AA}$ )	$b$ ( $\text{\AA}$ )	$c$ ( $\text{\AA}$ )			
$P6_3/mmc$	5.3599(2)	5.3599(2)	6.7647(3)	168.57	$\chi$ (300 K, 0.04 T) = 5.8	7.0
$Pnma$	6.7486(4)	5.1426(4)	9.7382(7)	337.97	$\chi$ (200 K, 0.04 T) = 5.2	5.9

the sharpening of the features associated with the transition upon annealing, and a dependence of the transition width and magnitude on the exact Y:In composition. All data presented here are for the Y:In = 2.2:1 annealed specimens, which showed the sharpest transition and the highest step in magnetization and resistivity. Powder neutron and x-ray diffraction at room temperature confirm the known  $P6_3/mmc$  structure of  $Y_2In$ . Additional temperature-dependent neutron-diffraction data were collected on the BT-1 powder diffractometer at the NIST Center for Neutron Research. Collimators of 15', 20', and 7' were used before and after the Cu (311) monochromator ( $\lambda = 1.5401\text{\AA}$ ) and after the sample, respectively, and data were collected in steps of  $0.05^\circ$  in the  $2\theta$  range of  $3^\circ$  to  $168^\circ$ . The results of the Rietveld structural refinements with the FULLPROF software of the data below ( $T = 200$  K) and above ( $T = 300$  K) the structural phase transition are summarized in Table I. Due to high air sensitivity of the samples, diffraction data were collected on a powder sample sealed under an inert atmosphere in a Pyrex tube. Complementary powder x-ray diffraction measurements using Cu  $K_\alpha$  radiation ( $\lambda = 1.5401\text{\AA}$ ) were carried out at several temperatures between 200 and 300 K in a Bruker diffractometer equipped with a liquid-nitrogen-cooled sample stage.

Temperature- and field-dependent dc magnetization measurements were performed in a Quantum Design (QD) Magnetic Property Measurement System for temperatures between 1.8 and 400 K, and for applied magnetic fields up to 7 T. Specific heat was measured from 2 to 100 K in a QD Physical Property Measurement System (PPMS). DC resistivity measurements from 2 to 300 K were carried out using the standard four-probe method in the QD PPMS in  $H = 0$ .

Band structure calculations were performed using the full-potential linearized augmented plane-wave method implemented in the WIEN2K package [36,37]. The Perdew-Burke-Ernzerhof generalized-gradient-approximation (PBE-GGA) exchange-correlation potential was used and a  $10 \times 10 \times 10$  grid was used to sample the  $k$  points in the Brillouin zone.

### III. RESULTS AND DISCUSSION

The magnetic ground states of  $R_2In$  compounds are diverse, ranging from antiferromagnets ( $R = Gd, Tb, Dy$ ) and ferromagnets ( $R = Ho, Er, Tm$ ) to weak diamagnets ( $R = Sm, Yb, Eu$ ) [38]. The magnetic susceptibility of  $Y_2In$  was previously reported to be temperature independent, and no transitions were observed in the temperature range between 4.2 and 300 K [38]. By contrast, our temperature-dependent magnetization data for  $Y_2In$  reveal a step around  $T_0 = 250$  K [Fig. 1(a)]. The slight upturn in the low-temperature susceptibility data points towards the presence of a small magnetic impurity, which amounts to 0.003% Gd. A well-pronounced thermal

hysteresis with a width of about 10 K, shown in the inset of Fig. 1(a), suggests that the  $T_0$  transition is first order [13–15]. Such a step has previously been observed in the magnetic susceptibility of a number of materials with structural phase transitions [1–6], some of which are accompanied by magnetic spin reorientations [18,39]. In order to check whether or not the transition has a magnetic component, field-dependent magnetization isotherms were measured at temperatures below and above the transition, as shown in Fig. 1(b). Both the  $T = 200$  K (blue circle) and  $T = 300$  K (red triangle) isotherms appear to be paramagnetic.

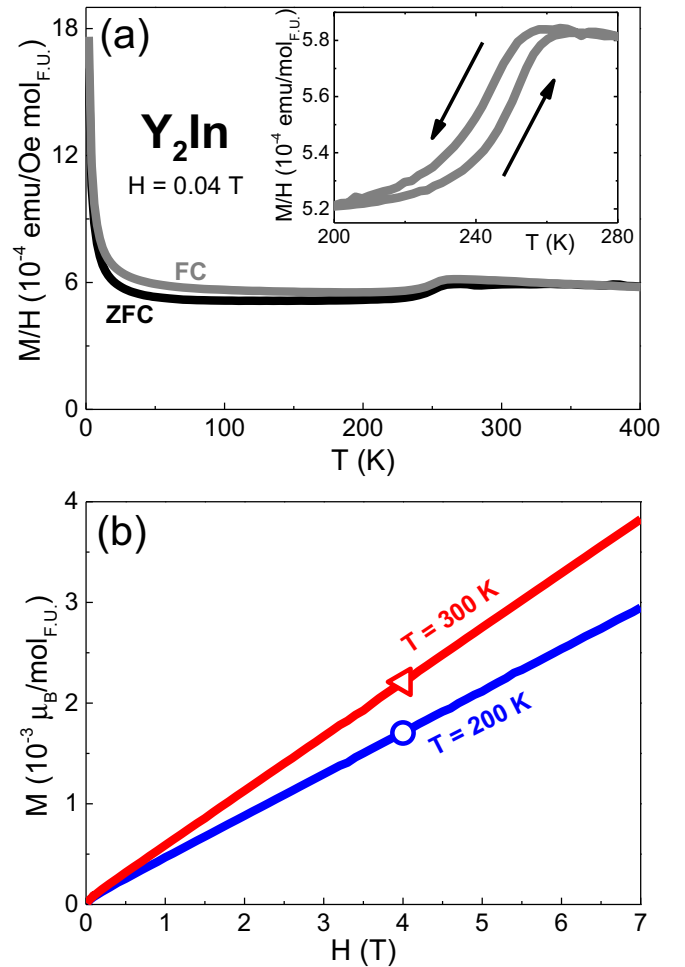


FIG. 1. (a) The zero-field-cooled (black line) and field-cooled (gray line) temperature-dependent magnetic susceptibility  $M(T)/H$  data of  $Y_2In$ , measured in  $H = 0.04$  T. Inset: the thermal hysteresis around the  $T_0 = 250 \pm 5$  K transition. [Note:  $1 \text{ emu}/(\text{mol}_{FU} \text{ Oe}) = 4\pi \cdot 10^{-6} \text{ m}^3/\text{mol}$ .] (b) Magnetization isotherms  $M(H)$ , measured at  $T = 200$  K (circle) and 300 K (triangle).

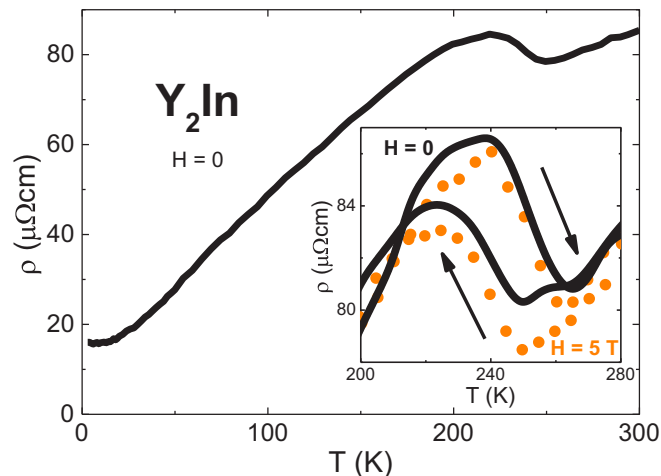


FIG. 2. The temperature-dependent resistivity  $\rho(T)$  of  $Y_2In$  in  $H = 0$ . Inset: the thermal hysteresis in  $H = 0$  (line) and  $H = 5$  T (symbols).

The temperature-dependent resistivity data (Fig. 2) support the possibility of a structural phase transition around  $T_0 = 250 \pm 5$  K. A hysteretic jump around  $T_0$  is observed in  $\rho(T)$  (Fig. 2) and is slightly broader ( $\Delta T \sim 10$  K) than the  $M(T)/H$  hysteresis. The resistivity enhancement associated with the transition  $\Delta\rho(T)/\rho(T) \approx 9\%$  is large and comparable to what had been observed for other structural phase transitions [1,2,16]. The small residual resistivity ratio, RRR =

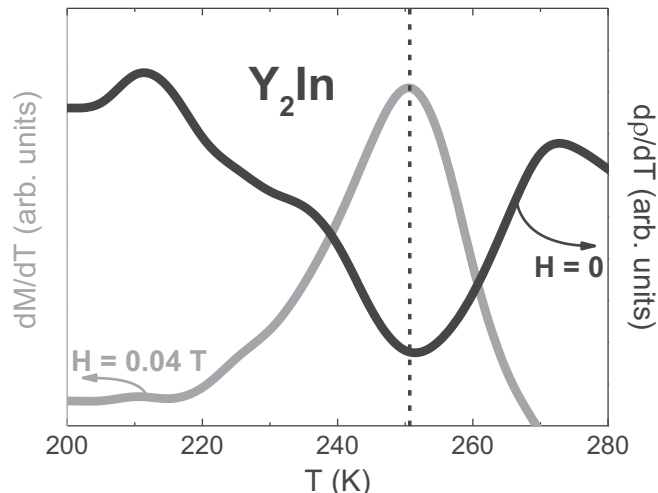


FIG. 3. The transition temperature  $T_0 = 250 \pm 5$  K, determined from the derivatives of susceptibility  $dM/dT$  ( $H = 0.04$  T, gray line, left axis) and resistivity  $d\rho/dT$  ( $H = 0$ , black line, right axis).

$\rho(300\text{ K})/\rho(2\text{ K}) = 5$ , can be attributed to the polycrystalline sample form. From the inset of Fig. 2, it is clearly seen that both the transition temperature  $T_0$  and the thermal hysteresis width are essentially unchanged with field, confirming the lack of a magnetic component. A better estimate of  $T_0$  is available from combined derivatives of susceptibility  $dM/dT$  (Fig. 3, gray line, left axis) and resistivity  $d\rho/dT$  (Fig. 3, black line,

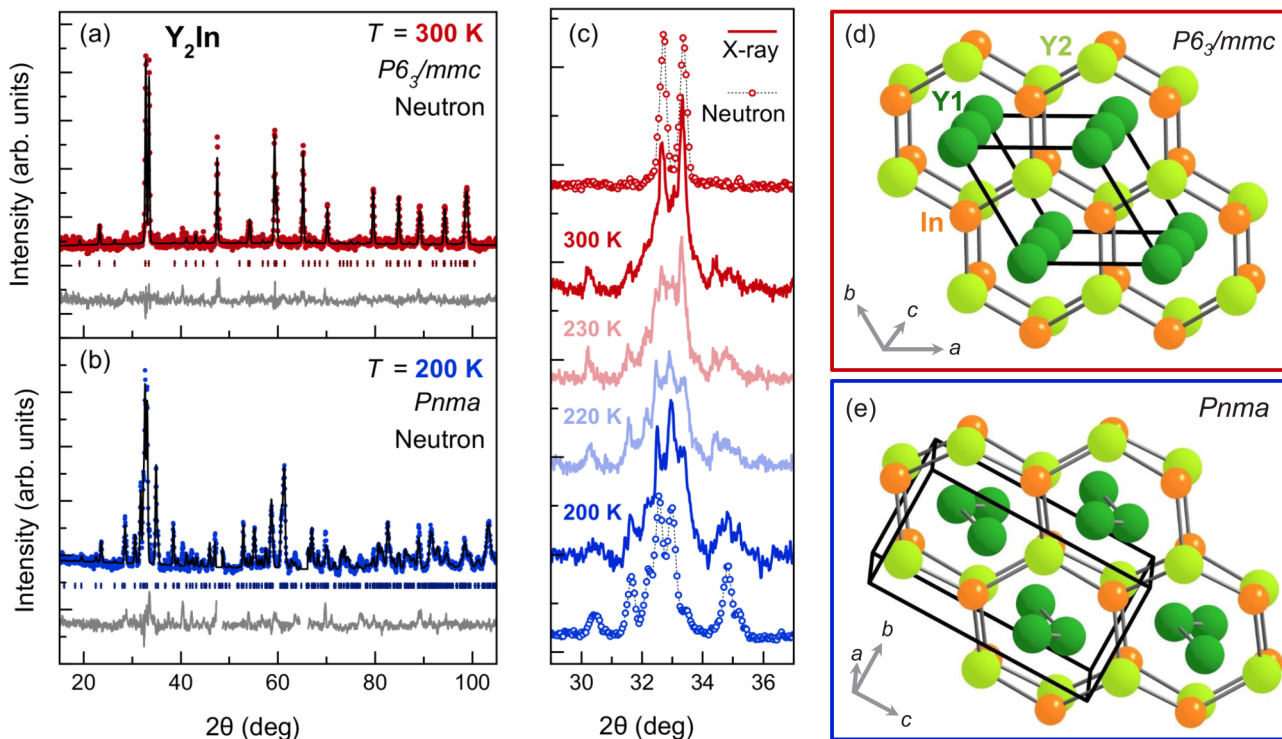


FIG. 4. Neutron-diffraction patterns of  $Y_2In$  (symbols) for (a)  $T = 300$  K and (b)  $T = 200$  K. The data were fit (black line) with (a)  $P6_3/mmc$  and (b)  $Pnma$  space groups, with calculated peak positions represented by the vertical symbols. The difference between the measured and fit data is shown as a gray line. (c) Evolution of the x-ray diffraction pattern (solid lines) between 200 and 300 K compared with the neutron data (symbols). The high- and low-temperature crystal structures are shown in (d)  $P6_3/mmc$  and (e)  $Pnma$ , with the unit cell outlined in black.

right axis), which give  $T_0 = 250 \pm 5$  K, where the uncertainty corresponds to the width of the hysteresis.

To further examine the nature of the steplike transition in  $Y_2\text{In}$ , structural analysis of the powder neutron-diffraction patterns was performed at temperatures above [ $T = 300$  K, Fig. 4(a)] and below [ $T = 200$  K, Fig. 4(b)]  $T_0$ . At high temperature,  $Y_2\text{In}$  forms in the hexagonal  $P6_3/mmc$  structure [Fig. 4(d)], consistent with previous reports [31,32]. Upon cooling through the  $T_0 = 250 \pm 5$  K transition, the structure changes to the orthorhombic  $Pnma$  [Fig. 4(e)], which has not been reported previously. The temperature evolution of this structural transition was studied with powder x-ray diffraction [Fig. 4(c)]. As the wavelengths of the neutron- and x-ray diffraction measurements are equivalent, the peak positions can be directly compared at  $T = 300$  and  $T = 200$  K, showing good agreement. However, the relative peak intensities cannot be directly compared due to the difference in the scattering interaction. At  $T = 300$  K, there are two prominent Bragg peaks between  $32^\circ$  and  $34^\circ$ , which are indexed as (102) and (110) in the  $P6_3/mmc$  space group. Cooling through the symmetry reducing structural transition, many new Bragg peaks emerge, including an intense reflection at  $33^\circ$ , which is indexed as (211) within the  $Pnma$  space group. The x-ray diffraction measurements at  $T = 230$  and  $T = 220$  K show a coexistence of Bragg reflections from both the high- and low-temperature phases, consistent with the interval of hysteresis shown in Fig. 1(a).

The nature of the structural transition in  $Y_2\text{In}$  can be understood by comparing the crystal structures, presented in Figs. 4(d) and 4(e), of the high-temperature hexagonal ( $P6_3/mmc$ ) and low-temperature orthorhombic ( $Pnma$ ) phases, respectively. In both structures, the indium atoms (orange) occupy a single crystallographic site and the yttrium atoms occupy two crystallographic sites [Y1 (dark green) and Y2 (light green)]. In the hexagonal case, the structure can be visualized as Y1 chains along the  $c$  axis, enclosed by a honeycomb of In and Y2 within the  $ab$  plane. Within the honeycomb lattice, the Y2–In distance is  $3.11 \text{ \AA}$ , while the adjacent honeycomb layers are separated by  $3.39 \text{ \AA}$ . In the orthorhombic structure, the Y1 atoms are displaced into a buckled chain, leading to an increased Y1–Y1 distance. The honeycomb of In and Y2 is also distorted, primarily along the  $a$  axis, with the Y1–In separation alternating between  $2.73$  and  $4.02 \text{ \AA}$ .

The experimental evidence for the structural transition at  $T_0$  motivated band structure calculations, which are shown in Fig. 5(a). The  $\text{DOS}(E_F)$  is larger for the high-temperature phase than the low-temperature phase. This is consistent with the observed drop in the Pauli susceptibility, with the respective  $\chi_0$  values listed in Table I. The  $d$ -electron contribution to the DOS shows a peak for the high-temperature phase, which then flattens out in the low-temperature phase (dashed lines). Both the total and partial DOS are similar to those calculated for  $\text{YCu}$  [30] and  $\text{LaCd}$  [28], two materials that undergo structural phase transition driven by the band Jahn-Teller

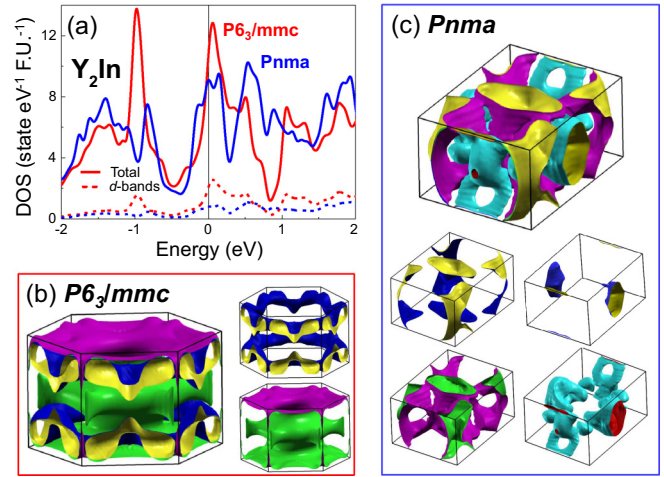


FIG. 5. (a) The total (solid line) and  $d$ -electron (dashed line) nonmagnetic density of states for the  $Pnma$  (blue line) and the  $P6_3/mmc$  (red line) phases of  $Y_2\text{In}$ . Fermi surface plots for the (b)  $P6_3/mmc$  and (c)  $Pnma$  phases of  $Y_2\text{In}$ .

mechanism. The number of bands contributing to the DOS ( $E_F$ ) is two for the high-temperature phase and four for the low-temperature phase, consistent with a lowered free energy [Figs. 5(b) and 5(c)].

It is important to note that the structural phase transition in  $Y_2\text{In}$  might be accompanied by the formation of a charge density wave. However, a definitive analysis is only possible for single crystals, which are currently not available.

#### IV. CONCLUSIONS

It was found that  $Y_2\text{In}$  exhibits a structural phase transition at  $T_0 = 250 \pm 5$  K, as evidenced by crystallographic analysis, magnetization, and resistivity data. The phase transition from a high-temperature hexagonal  $P6_3/mmc$  to a low-temperature orthorhombic  $Pnma$  phase is accompanied by a large thermal hysteresis of about 10 K, indicating that this transition is first order. Based on band structure calculations, this structural phase transition can likely be attributed the band Jahn-Teller effect. The possibility of an accompanying charge density wave formation has not been ruled out and is left to a future study.

#### ACKNOWLEDGMENT

The authors acknowledge fruitful discussions with Z. Fisk and R. Robinson. The work at Rice University was supported by Grant No. NSF DMR-1506704.

The identification of any commercial product or trade name does not imply endorsement or recommendation by the National Institute of Standards and Technology.

- [1] N. Ni, S. Nandi, A. Kreyssig, A. I. Goldman, E. D. Mun, S. L. Bud'ko, and P. C. Canfield, *Phys. Rev. B* **78**, 014523 (2008).  
 [2] G. Wu, H. Chen, T. Wu, Y. L. Xie, Y. J. Yan, R. H. Liu, X. F. Wang, J. J. Ying, and X. H. Chen, *J. Phys.: Condens. Matter* **20**, 422201 (2008).

- [3] H. Balster, H. Ihrig, A. Kockel, and S. Methfessel, *Z. Phys. B* **21**, 241 (1975).  
 [4] H. Kadomatsu, Y. Kawanishi, M. Kurisu, T. Tokunaga, and H. Fujiwara, *J. Less Common Metals* **141**, 29 (1988).

- [5] M. Tegel, M. Rotter, V. Weiss, F. M. Schappacher, R. Poettgen, and D. Johrendt, *J. Phys.: Condens. Matter* **20**, 452201 (2008).
- [6] E. L. Semenova and Y. Kudryavtsev, *J. Alloys Compd.* **203**, 165 (1994).
- [7] M. Kurisu, *J. Phys. Soc. Jpn.* **56**, 4064 (1987).
- [8] K. Yagasaki, Y. Uwatoko, Y. Fadena, H. Fujii, and T. Okamoto, *J. Phys. F* **15**, 651 (1985).
- [9] H. Ihrig and W. Lohmann, *J. Phys. F* **7**, 1957 (1977).
- [10] A. Asamitsu, Y. Moritomo, Y. Tomioka, T. Arima, and Y. Tokura, *Nature (London)* **373**, 407 (1995).
- [11] A. Asamitsu, Y. Moritomo, R. Kumai, Y. Tomioka, and Y. Tokura, *Phys. Rev. B* **54**, 1716 (1996).
- [12] K. A. Muller and H. Thomas, *Structural Phase Transitions* (Springer-Verlag, New York, 1991).
- [13] Y. Mnyukh, *Am. J. Condens. Matter Phys.* **3**, 25 (2013).
- [14] S. Ohkoshi, T. Matsuda, H. Tokoro, and K. Hashimoto, *Chem. Mater.* **17**, 81 (2005).
- [15] D. G. Thomas and L. A. Staveley, *J. Chem. Soc.* **573**, 2572 (1951).
- [16] J. Q. Yan, S. Nandi, B. Saparov, P. Čermák, Y. Xiao, Y. Su, W. T. Jin, A. Schneidewind, T. Brückel, R. W. McCallum, T. A. Lograsso, B. C. Sales, and D. G. Mandrus, *Phys. Rev. B* **91**, 024501 (2015).
- [17] Y. Gefen and M. Rosen, *Scr. Metall.* **14**, 645 (1980).
- [18] S. Li, C. de la Cruz, Q. Huang, Y. Chen, J. W. Lynn, J. Hu, Y.-L. Huang, F.-C. Hsu, K.-W. Yeh, M.-K. Wu, and P. Dai, *Phys. Rev. B* **79**, 054503 (2009).
- [19] O. Jung, D. Jo, Y. Lee, B. Conklin, and C. G. Pierpont, *Inorg. Chem.* **36**, 19 (1997).
- [20] T. Furubayashi, T. Matsumoto, T. Hagino, and S. Nagata, *J. Phys. Soc. Jpn.* **63**, 3333 (1994).
- [21] T. R. McGuire and C. J. Kriessman, *Phys. Rev.* **85**, 452 (1952).
- [22] C. S. Lue, Y.-K. Kuo, F. H. Hsu, H. H. Li, H. D. Yang, P. S. Fodor, and L. E. Wenger, *Phys. Rev. B* **66**, 033101 (2002).
- [23] G. Grüner, *Rev. Mod. Phys.* **60**, 1129 (1988).
- [24] N. S. Sangeetha, A. Thamizhavel, C. V. Tomy, S. Basu, A. M. Awasthi, P. Rajak, S. Bhattacharyya, S. Ramakrishnan, and D. Pal, *Phys. Rev. B* **91**, 205131 (2015).
- [25] J. N. Lalena and D. A. Cleary, *Principles of Inorganic Materials Design* (Wiley-Interscience, New York, 2005).
- [26] P. J. Brown, A. Y. Bargawi, J. Crangle, K. U. Neumann, and K. R. Ziebeck, *J. Phys.: Condens. Matter* **11**, 4715 (1999).
- [27] S. K. Ghatak, D. K. Ray, and C. Tannous, *Phys. Rev. B* **18**, 5379 (1978).
- [28] S. Asano and S. Ishida, *J. Phys. Soc. Jpn.* **54**, 4241 (1985).
- [29] S. Fujii, S. Ishida, and S. Asano, *J. Phys. Soc. Jpn.* **58**, 3657 (1989).
- [30] Y. J. Shi, Y. L. Du, G. Chen, and G. L. Chen, *Phys. Lett. A* **368**, 495 (2007).
- [31] E. Franceschi, *J. Less-Common Met.* **37**, 157 (1974).
- [32] A. Palenzona, *J. Less-Common Met.* **16**, 379 (1968).
- [33] M. L. Fornasini and S. Cirafici, *Z. Kristallog.* **190**, 295 (1990).
- [34] O. D. McMasters, C. L. Nipper, and K. A. Gschneidner, *J. Less-Common Met.* **23**, 253 (1970).
- [35] S. Curtarolo, W. Setyawan, S. Wang, J. Xue, K. Yang, R. H. Taylor, L. J. Nelson, G. L. W. Hart, S. Sanvito, M. Buongiorno-Nardelli, N. Mingo, and O. Levy, *Comput. Mater. Sci.* **58**, 227 (2012).
- [36] P. K. Blaha, K. Schwarz, G. Madsen, D. Kvasnicka, and J. Luitz, computer code WIEN2K package, <http://www.wien2k.at> (2001).
- [37] J. P. Perdew, K. Burke, and M. Ernzerhof, *Phys. Rev. Lett.* **77**, 3865 (1996).
- [38] H. Gamari-Seale, T. Anagnostopoulos, and J. K. Yakinthos, *J. Appl. Phys.* **50**, 434 (1979).
- [39] A. Yamada and M. Tanaka, *Mater. Res. Bull.* **30**, 715 (1995).

*Correction:* The omission of an acknowledgment statement has been fixed.